Supplementary Figures S1–S4 supporting the Information Flow analysis presented in the main manuscript.

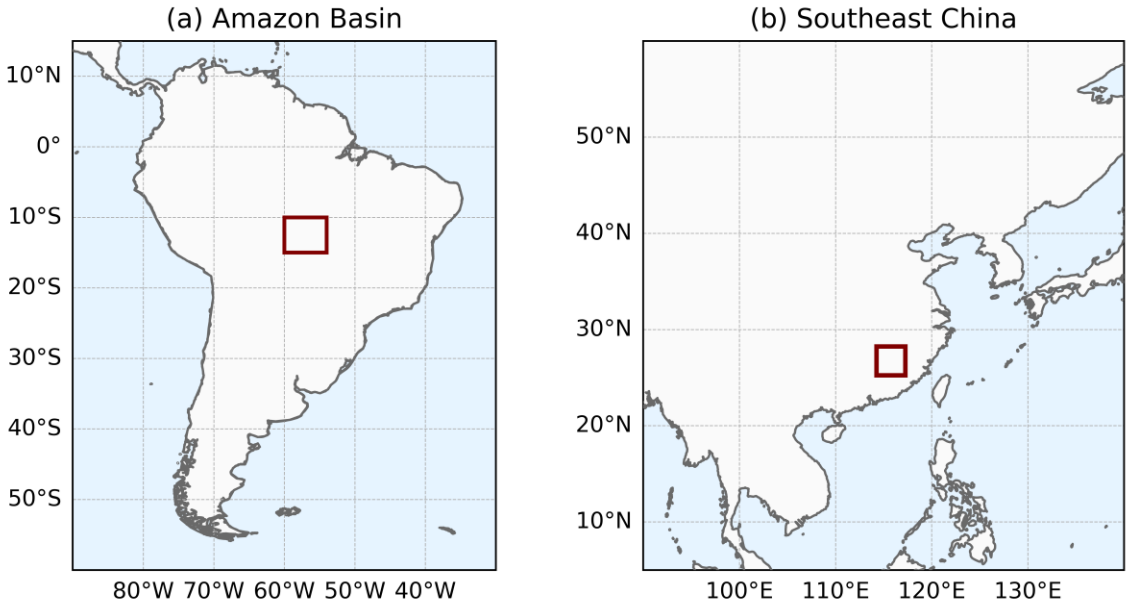

Fig. S1. Location of the two humid-forest study regions. (a) Amazon Basin (54–60°W, 10–15°S) and (b) southeast China (114.25–117.25°E, 25.25–28.25°N).


(a)
SM→LAI
VPD→LAI
SM→GPP
VPD→GPP
(b)
SM→LAI
VPD→LAI
SM→GPP
VPD→GPP
ΔIF_2
ΔIF_3
(c)
ΔIF_1
ΔIF_2
ΔIF_3
SM→LAI
VPD→LAI
SM→GPP
VPD→GPP
SM_Q1×VPD_Q1
SM_Q1×VPD_Q4
SM_Q4×VPD_Q1
SM_Q4×VPD_Q4

Fig. S2. ΔInformation Flow (ΔIF) for SM→LAI, VPD→LAI, SM→GPP, and VPD→GPP across combined quartiles of soil moisture (SM) and vapor pressure deficit (VPD) for southeast China. Each panel illustrates how ΔIF varies across environmental regimes defined by water supply (SM: Q1–Q4) and atmospheric demand (VPD: Q1–Q4), shown for three conditioning levels.

(a) ΔIF_1, computed as the difference between the bivariate IF and the IF conditioned only on the paired driver (i.e., SM conditioned on VPD, or VPD conditioned on SM).

(b) ΔIF_2 and ΔIF_3, computed as the difference between the bivariate IF and the IF conditioned on the paired driver and temperature (SM/VPD and T/R respectively).

(c) ΔIF_1, ΔIF_2 and ΔIF_3 represent the differences between the bivariate IF and the multivariate IF under three conditioning schemes.

ΔIF_1: SM→LAI/GPP conditioned on VPD, and VPD→LAI/GPP conditioned on SM;

ΔIF_2: SM→LAI/GPP or VPD→LAI/GPP conditioned on the paired driver and temperature (SM/VPD + T);

ΔIF_3: SM→LAI/GPP or VPD→LAI/GPP conditioned on the paired driver, temperature, and solar surface radiation (SM/VPD + T + SSR).

Across all panels, bar heights indicate the magnitude of ΔIF for each SM–VPD quartile combination, with error bars showing the 95% confidence interval. These supplementary plots provide a detailed view of how ΔIF responds to changing hydroclimatic conditions and mediator configurations, complementing the combined rIF–ΔIF diagnostic presented in Figure 4.

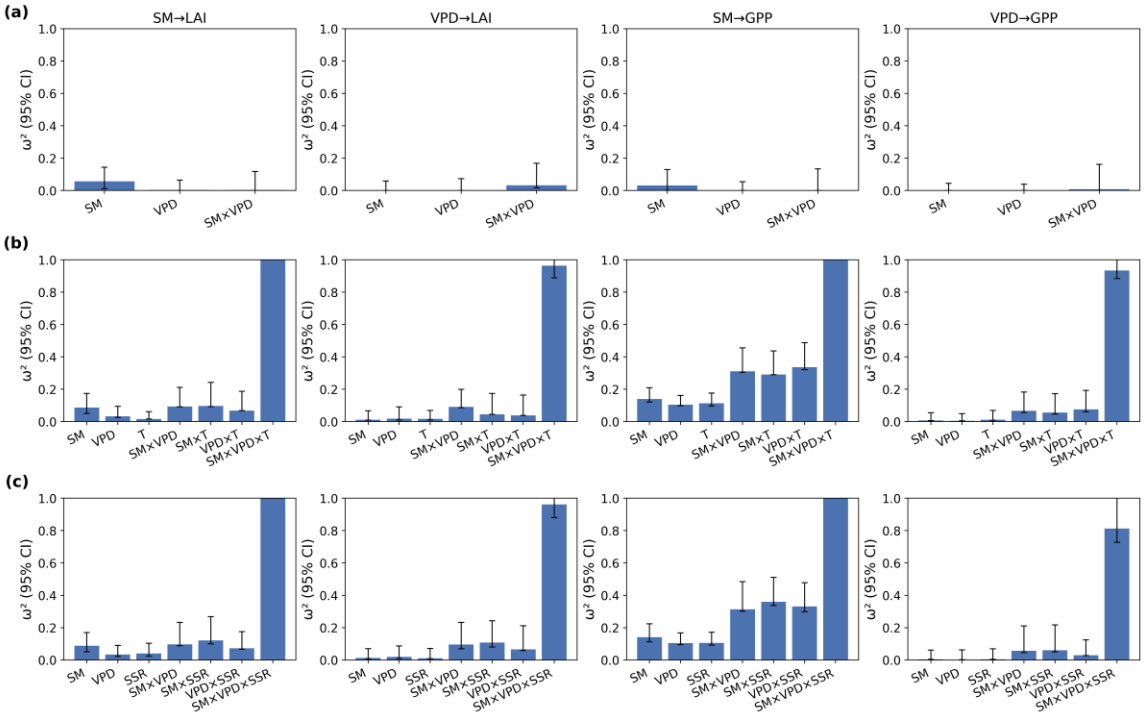

Fig. S3. Fraction of variance (ω²) for |ΔIF| attributed to each ANOVA factor and interaction, corresponding to the same regime structures used in Fig. 5. Bars show the relative dominance of soil moisture (SM), vapor-pressure deficit (VPD), temperature (T), solar radiation (SSR), and their interactions in explaining variability in |ΔIF| across pathways.

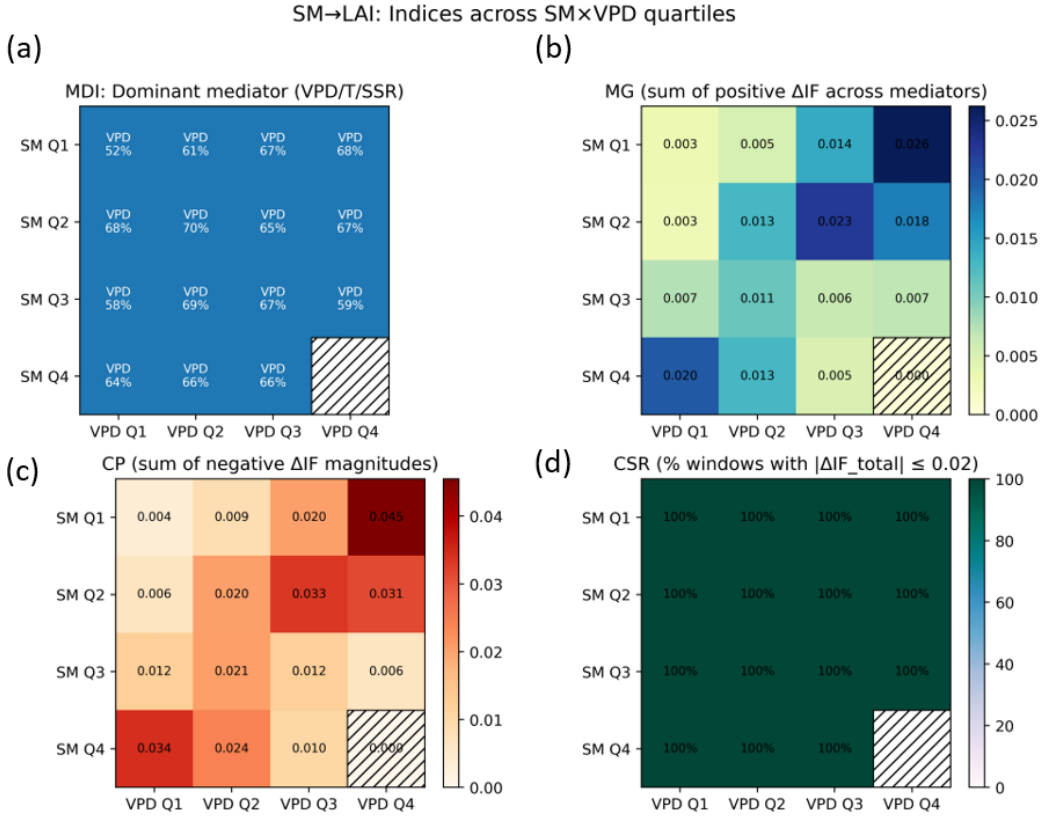
SM→LAI: Indices across SM×VPD quartiles
(a)
MDI: Dominant mediator (VPD/T/SSR)
SM Q1
SM Q2
SM Q3
SM Q4
VPD Q1
VPD Q2
VPD Q3
VPD Q4
VPD 52%
VPD 61%
VPD 67%
VPD 68%
VPD 68%
VPD 70%
VPD 65%
VPD 67%
VPD 58%
VPD 69%
VPD 67%
VPD 59%
VPD 64%
VPD 66%
VPD 66%
(b)
MG (sum of positive ΔIF across mediators)
0.003
0.005
0.014
0.026
0.003
0.013
0.023
0.018
0.007
0.011
0.006
0.007
0.020
0.013
0.005
0.000
0.025
0.020
0.015
0.010
0.005
0.000
(c)
CP (sum of negative ΔIF magnitudes)
0.004
0.009
0.020
0.045
0.006
0.020
0.033
0.031
0.012
0.021
0.012
0.006
0.034
0.024
0.010
0.000
0.04
0.03
0.02
0.01
0.00
(d)
CSR (% windows with |ΔIF_total| ≤ 0.02)
100%
100
80
60
40
20
0

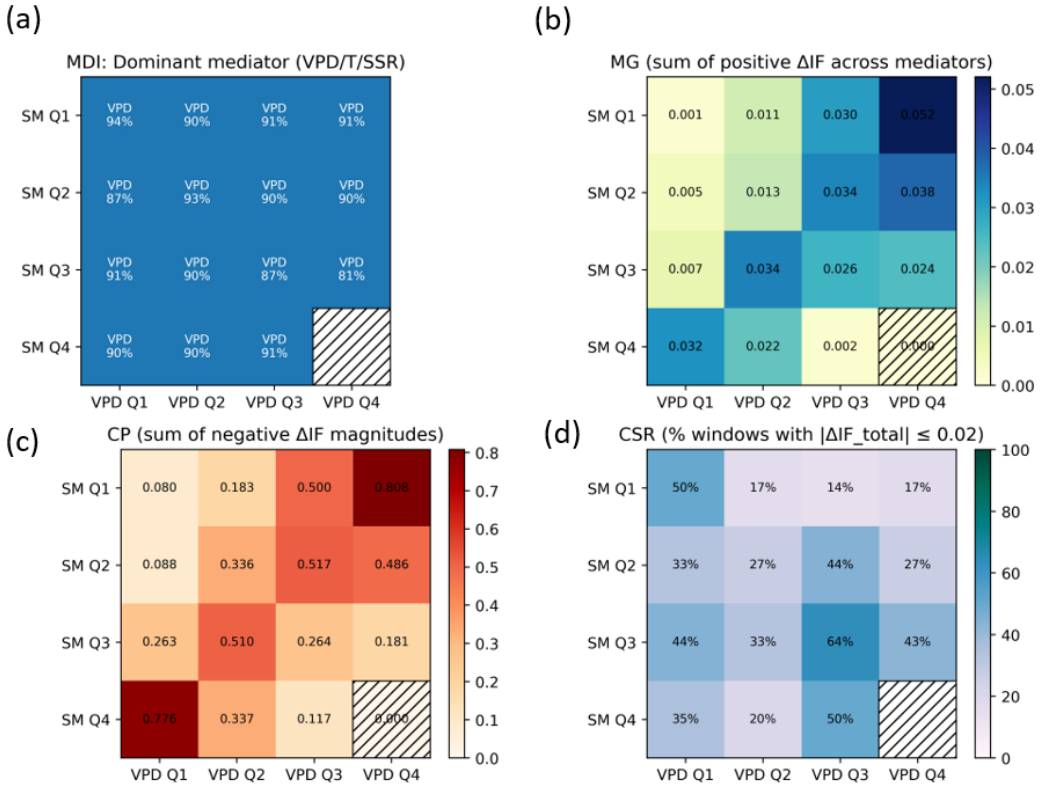
SM→GPP: Indices across SM×VPD quartiles
(a)
MDI: Dominant mediator (VPD/T/SSR)
SM Q1
SM Q2
SM Q3
SM Q4
VPD Q1
VPD Q2
VPD Q3
VPD Q4
VPD 94%
VPD 90%
VPD 91%
VPD 91%
VPD 87%
VPD 93%
VPD 90%
VPD 90%
VPD 91%
VPD 90%
VPD 87%
VPD 81%
VPD 90%
VPD 90%
VPD 91%
(b)
MG (sum of positive ΔIF across mediators)
0.001
0.011
0.030
0.052
0.005
0.013
0.034
0.038
0.007
0.034
0.026
0.024
0.032
0.022
0.002
0.000
0.05
0.04
0.03
0.02
0.01
0.00
(c)
CP (sum of negative ΔIF magnitudes)
0.080
0.183
0.500
0.808
0.088
0.336
0.517
0.486
0.263
0.510
0.264
0.181
0.776
0.337
0.117
0.000
0.8
0.7
0.6
0.5
0.4
0.3
0.2
0.1
0.0
(d)
CSR (% windows with |ΔIF_total| ≤ 0.02)
50%
17%
14%
17%
33%
27%
44%
27%
44%
33%
64%
43%
35%
20%
50%
100
80
60
40
20
0

Fig. S4. Mediator-decomposition indices (a: mediator dominance; b: moderation gain; c: confounding pressure; d: causal sufficiency rate) evaluated separately across all SM–VPD quartile regimes for the SM→LAI and SM→GPP pathways.

These panels complement Fig. 6 by illustrating how the importance of mediators varies across distinct hydroclimatic conditions.